Holes and chaotic pulses of traveling waves coupled to a long-wave mode

Henar Herrero

Departamento de Matemáticas, Facultad de Ciencias Químicas, Universidad de Castilla-La Mancha, 13071 Ciudad Real, Spain

Hermann Riecke

Department of Engineering Sciences and Applied Mathematics, Northwestern University, Evanston, IL 60208, USA

Abstract

Localized traveling-wave pulses and holes, i.e. localized regions of vanishing wave amplitude, are investigated in a real Ginzburg-Landau equation coupled to a long-wave mode. In certain parameter regimes the pulses exhibit a Hopf bifurcation which leads to a breathing motion. Subsequently the oscillations undergo period-doubling bifurcations and become chaotic.

PACS: 47.20.ky, 47.27.te, 05.45.+b, 85.30.De.

Keywords: chaos, localized patterns.

Over the past few years localized structures have been investigated in a number of pattern-forming systems, as varied as semiconductor devices [1,2], electric gas discharges [3], binary fluid convection [4–6], convection in narrow channels [7] etc. Among them are structures consisting of domains of different wavenumbers [7–9]. In particular, the localized traveling-wave patterns ('pulses') observed in binary-fluid convection have found considerable interest [4–6,10–15]. The experimental results [4–6] lead to a number of theoretical analyses aimed at an understanding of the mechanism of localization. Within the framework of a single complex Ginzburg-Landau equation dispersion was identified as an important ingredient for localization [10–12]. It was, however, recognized that this equation does not suffice to explain various qualitative features of the pulses. The inclusion of a coupling of the traveling waves to an additional long-wave mode lead to a detailed understanding of a number of qualitative features of the pulses [13–15]. Equations of similar type as the resulting extended Ginzburg-Landau equations have been investigated in the context of two-layer Poiseuille flow [16] and should apply more generally to the interaction of traveling waves with a long-wave mode, e.g. in capillary jets with thermocapillarity [17].

In the present paper we investigate the extended Ginzburg-Landau equations further and focus on two types of localized structures: periodically and aperiodically oscillating ('bright') pulses, and 'holes' or 'dark pulses', i.e. stable localized domains of the basic state within the traveling-wave state. In a previous paper the pulses were described within the framework of two interacting fronts each connecting the stable basic state with the coexisting stable traveling-wave state [14]. A simple mechanism was identified which leads to an interaction between the fronts. This interaction depends strongly on the direction of propagation of the pulse. In the context of binary-mixture convection it implied that these pulses are only stable if they propagate opposite to their (linear) group velocity. Simple arguments suggest that the localization mechanism should not only stabilize pulses but also holes. We confirm this numerically in the present paper. The asymptotic analysis used in [14] only applies to *steadily* propagating pulses. Here we study numerically the regime outside the validity of that analysis and find pulses which propagate unsteadily, with periodically and aperiodically varying velocities. The phenomenon is quite similar to layer oscillations found in reaction-diffusion models [18,19].

The extended Ginzburg-Landau equations introduced in Ref. [13,20] in the context of binary-mixture convection are given to cubic order by

$$\partial_t A + (s + s_2 C)\partial_x A = d\partial_x^2 A + (a + fC + f_2 C^2 + f_3 \partial_x C)A + cA|A|^2 + ..., \tag{1}$$

$$\partial_t C = \delta \partial_x^2 C - \alpha C + h^{(2)} \partial_x |A|^2 + (h^{(1)} + h^{(3)} C)|A|^2 + \\ i h^{(4)} (A^* \partial_x A - A \partial_x A^*) + ... \tag{2}$$

Here the amplitude A denotes the traveling-wave amplitude and corresponds to that appearing in the conventional Ginzburg-Landau equation, and C characterizes a non-oscillatory, long-wave mode. In binary-mixture convection the long-wave mode corresponds to a large-scale concentration field. Due to the wave character of the amplitude A the long-wave mode cannot only be generated by A but also advected. For that reason - and because of the group velocity - equations (1,2) are not of reaction-diffusion type.

As in the asymptotic analysis in [14] we neglect dispersion and assume all the coefficients to be real in order to focus on the effect of the long-wave mode. To allow an analytical treatment of the interaction of fronts a limit of weak diffusion was considered in [14] which lead to

$$\partial_t A + \eta^2 s_2 \partial_x A = \eta^2 d_2 \partial_x^2 A - A + cA^3 - A^5 + CA, \tag{3}$$

$$\partial_t C = \eta^4 \delta_4 \partial_x^2 C - \eta^2 \alpha_2 C + \eta^3 h_3^{(2)} \partial_x A^2 + \eta^2 h_2^{(3)} C A^2, \tag{4}$$

with $\eta \ll 1$. The terms involving $h^{(1)}$ and $h^{(4)}$ were omitted since these coefficients turned out to vanish in the case considered in [14]. The equations were rescaled such that the bifurcation parameter - which is related to the Rayleigh number in convection - is the coefficient of the cubic term c. The limit $\eta \ll 1$ allowed the derivation of coupled evolution equations for the velocities $v_{l,t}$ of the leading and trailing front, respectively, which together make up a pulse,

$$v_l = s_2 - \frac{\gamma}{|v_l|} + sgn(v_l)\rho, \tag{5}$$

$$v_t = s_2 - \frac{\gamma}{|v_t|} + 2\gamma \frac{e^{-\hat{\alpha} L/|v_l|}}{|v_l|} - sgn(v_t)\rho, \tag{6}$$

$$\partial_T L = \gamma \left(\frac{1}{v_t} - \frac{1}{v_l} \right) - 2\gamma \frac{e^{-\hat{\alpha} L/|v_l|}}{v_l} + 2\rho. \tag{7}$$

In (5,6,7) the length of the pulse is denoted by L and

$$\gamma = \sqrt{3} h_3^{(2)}, \quad \rho = \frac{\sqrt{3}}{\eta}(c - 4/\sqrt{3}), \quad T = \eta^2 t, \quad \hat{\alpha} = \alpha_2 - h_2^{(3)} A_0^2. \tag{8}$$

Since in (3,4) the diffusive term was considered much smaller than the advection term the interaction is one-sided, i.e. while the leading front is independent of the trailing front the latter feels the effect of the leading front. Therefore the peak in the long-wave mode

generated by the trailing front is reduced as compared to that of the leading front. For $h^{(2)} > 0$ this implies a repulsive interaction of the fronts and allows the pulse to be stable if the pulse velocity is opposite to the group velocity [14]. This argument suggests that backward drifting holes should be stable as well (for $h^{(2)} > 0$). It should be noted that for (5,6,7) to be valid, the front velocities cannot be too small. In particular, they cannot change sign.

To investigate the stability of holes, i.e. of localized domains with vanishing amplitude A, we solve (3,4) for $\eta = 1$ numerically using a Crank-Nicholson scheme. We use a system with periodic boundary conditions and a length $L = 50$. The steep gradients in C require a small grid spacing ($dx = 0.025$). The very slow dynamics allows large time steps ($dt = 1$). As expected from the asymptotic analysis, holes are indeed stable in a range of parameters. Their lengths are shown in fig. 1 (solid symbols) along with those of pulses (open symbols). The behavior of the holes is opposite to that of the pulses: their length increases with decreasing c and diverges below a critical value. The region of existence of stable holes as well as that of pulses decreases with increasing δ, i.e. with increasing diffusion of the long-wave mode. Above a critical value of δ no stable holes or pulses are found.

In the weak diffusion limit of the asymptotic analysis the leading front decouples from the trailing front and its velocity is independent of the location of the trailing front. For finite diffusion, however, the leading front is affected by the trailing front and therefore both fronts interact with each other. As a consequence, more complex dynamics can be expected. We now investigate this effect of increased diffusion on the dynamics of pulses using the same numerical procedure. When, for sufficiently strong diffusion, the control parameter c is decreased a Hopf bifurcation takes place and the length and velocity of the pulse start to oscillate, with the fronts oscillating in antiphase. Decreasing the parameter further three period-doubling bifurcations are found to occur, leading to a period 8 at $c = 2.561383$ (see figs.2 and 3). For $c = 2.561380$ we observe a period 6. For $c = 2.561340$ the dynamics become apparently chaotic as demonstrated in the Fourier spectrum shown in fig.4. The corresponding evolution of the pulse is shown in fig.5 which presents a space-time diagram of the location of the two fronts making up the pulse. Beyond this regime the dynamics become periodic again ($c = 2.561320$). Eventually, for $c < 2.561310$ the pulse loses stability and grows to fill the whole system.

For weak diffusion the (steady) pulses are unstable for positive velocity (in the case $h^{(2)} > 0$) [14] since the interaction between the fronts is attractive in that case. Strikingly,

for stronger diffusion the speed of the steady pulses decreases rapidly when c is decreased toward the lower end of the regime of stability (see fig. 6); in the oscillatory pulses that arise for still smaller c the instantaneous velocity can change signand the stable pulse propagates forward over parts of the oscillatio cycle. In fact, in this regime even the average velocity can be positive (cf. fig.5).

The oscillations shown in figs. 2 and 5 are very similar to the breathing motion of localized structures found in reaction-diffusion systems [18,19]. They can be periodic [18] or chaotic [19]. The systems studied in [18,19] differ, however, in various aspects from that discussed here. Eqs.(1,2) are not of reaction-diffusion type since the coupling occurs *via* the advection of the long-wave mode C by the traveling-wave mode A. Thus, the drift of the pulses (or holes) is an important feature and - at least for steady pulses - is closely related to their stability. In addition, in [19] Neumann boundary conditions were used and the distance between the two fronts making up the pulse was comparable to their distance from the boundaries. Thus, the boundaries may well play an important role in the dynamics. In the simulations presented here, the system was chosen long enough to ensure that the (periodic) boundary conditions are not important. Finally, one of the three reacting components of the system studied in [19] was assumed to diffuse very fast providing essentially a uniform background field which gives some aspect of a global coupling.

It should be mentioned that within the single complex Ginzburg-Landau equation pulses exhibiting complex dynamics have been found as well [21]. In contrast to the pulses discussed here, these pulses are short and stabilized by dispersion [11,12,15]. Their dynamics is related more to deformations in the pulse shape - presumably due to phase slips - than to the size of the pulse.

In conclusion we have extended the previous analysis of fronts and pulses of traveling waves coupled to a long-wave mode [14,22]. Numerically, we find that not only pulses but also holes (‘dark pulses’) can be stabilized by the long-wave mode. In addition, for sufficiently strong diffusion the mutual interaction between the leading and the trailing front of the pulses can lead to periodic as well as to aperiodic oscillations in the velocity and width of the pulses. No oscillatory holes have been found.

This work was supported by DOE through grant DE-FG02-92ER14303, by an equipment grant from NSF (DMS-9304397) and by the DGICYT (Spanish Government) under grant PB93-0708.

REFERENCES

[1] F.-J. Niedernostheide, M. Arps, R. Dohmen, H. Willebrand and H.-G. Purwins, Phys. Status Solidi B **172**, 249 (1992).

[2] E. Schöll and D. Drasdo, Z. Phys. B **81**, 183 (1990).

[3] E. Ammelt, D. Schweng and H.-G. Purwins, Phys. Lett. A **179**, 348 (1993).

[4] P. Kolodner, D. Bensimon, and C. Surko, Phys. Rev. Lett. **60**, 1723 (1988).

[5] J. Niemela, G. Ahlers, and D. Cannell, Phys. Rev. Lett. **64**, 1365 (1990).

[6] P. Kolodner, Phys. Rev. E **50**, 2731 (1994).

[7] J. Hegseth, J. Vince, M. Dubois, and P. Bergé, Europhys. Lett. **17**, 413 (1992).

[8] H. Brand and R. Deissler, Phys. Rev. Lett. **63**, 508 (1989).

[9] G. Granzow and H. Riecke, Phys. Rev. Lett. **77**, 2451 (1996).

[10] O. Thual and S. Fauve, J. Phys. (Paris) **49**, 1829 (1988).

[11] B. Malomed and A. Nepomnyashchy, Phys. Rev. A **42**, 6009 (1990).

[12] V. Hakim and Y. Pomeau, Eur. J. Mech. B Suppl **10**, 137 (1991).

[13] H. Riecke, Phys. Rev. Lett. **68**, 301 (1992).

[14] H. Herrero and H. Riecke, Physica D **85**, 79 (1995).

[15] H. Riecke and W.-J. Rappel, Phys. Rev. Lett. **75**, 4035 (1995).

[16] M. Renardy and Y. Renardy, Phys. Fluids **5**, 2738 (1993).

[17] J.-J. Xu and S.H. Davis. J. Fluid Mech. **161**, 1 (1985).

[18] Y. Nishiura and M. Mimura, SIAM J. Appl. Math. **49**, 481 (1989).

[19] M. Suzuki, T. Ohta, M. Mimura, and H. Sakaguchi, Phys. Rev. E **52**, 3645 (1995).

[20] H. Riecke, Physica D **92**, 69 (1996).

[21] R. Deissler and H. Brand, Phys. Rev. Lett. **72**, 478 (1994).

[22] H. Herrero and H. Riecke, Int. J. Bif. and Chaos **4**, 1343 (1994).

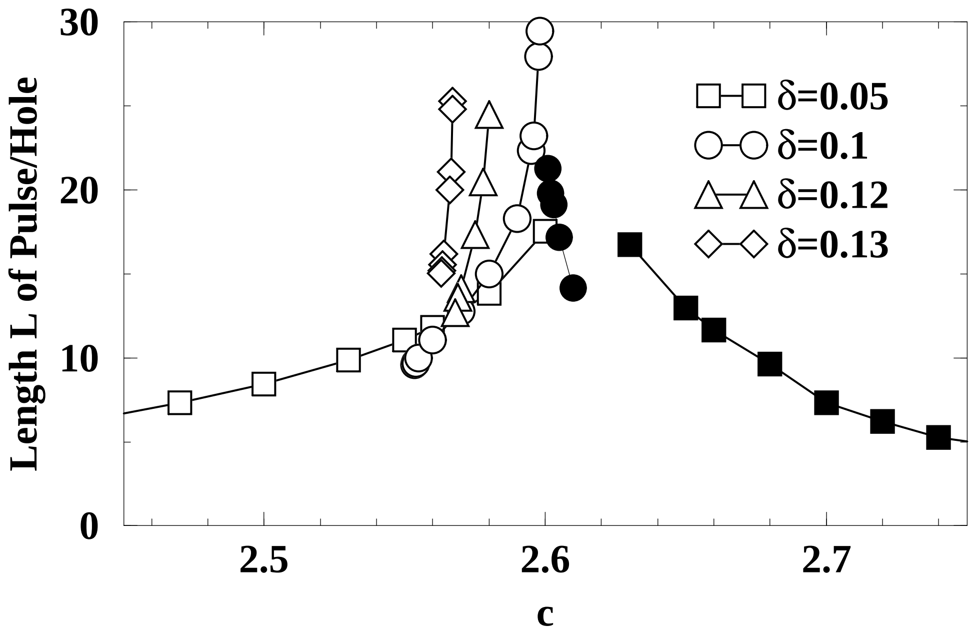

FIG. 1. Length of pulses (open symbols) and of holes (solid symbols) for different values of the diffusion coefficient of the long-wave mode. Open and solid squares correspond to $\delta = 0.05$; open and solid circles to $\delta = 0.1$. The remaining parameters are $s = 0.3$, $d = 0.05$, $\alpha = 0.01$, $h^{(2)} = 0.03$.

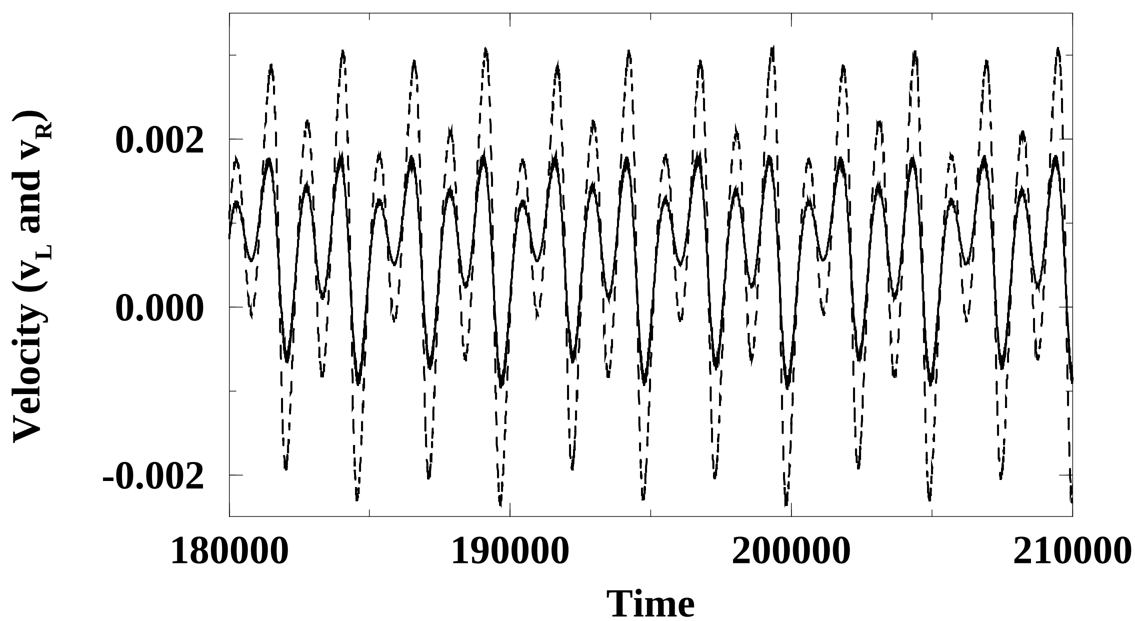

FIG. 2. Velocity of the left and right fronts that form the pulse for $c = 2.561383$ and $\delta = 0.13$ (period-8 regime). The remaining parameters are as in fig.1. The dashed line corresponds to the right front and the continuous line to the left one.

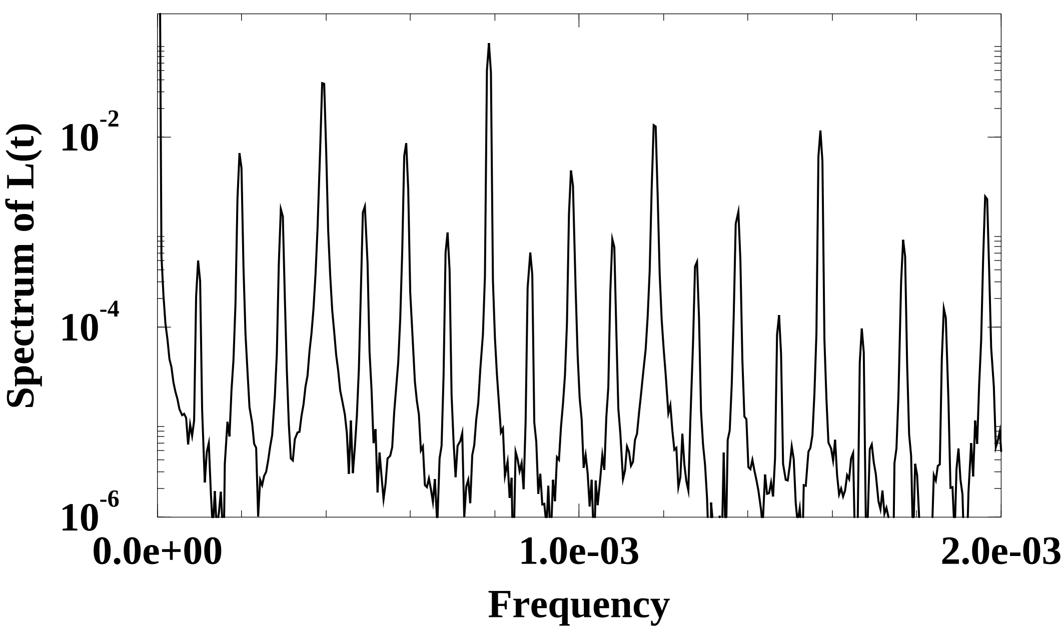

FIG. 3. Fourier spectrum of the length of the pulse for $c = 2.561383$ and $\delta = 0.13$ (period-8 regime). The remaining parameters are as in fig.1.

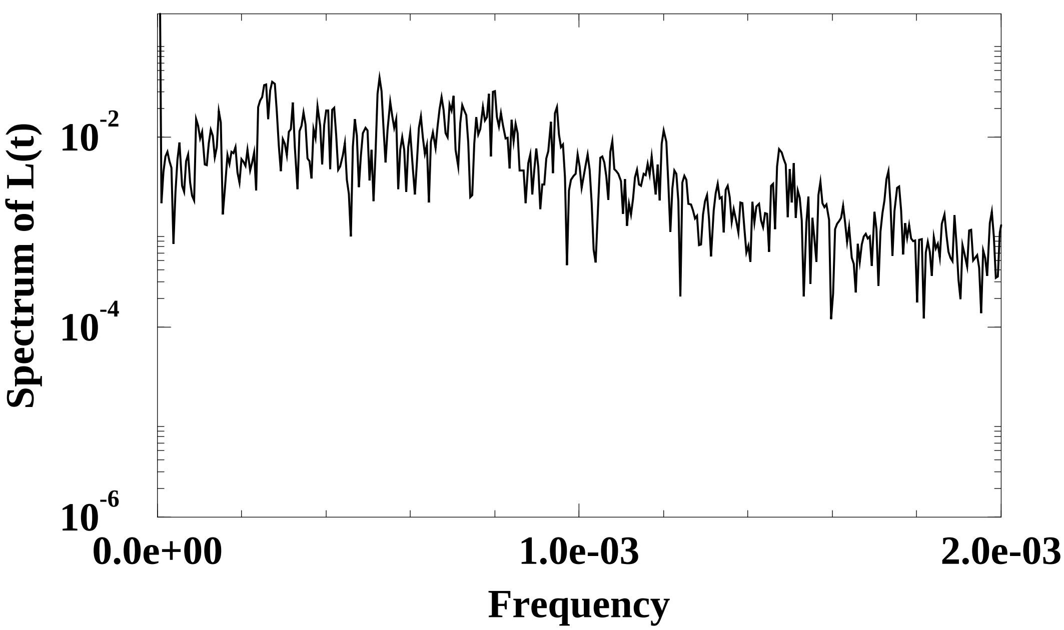

FIG. 4. Fourier spectrum of the length of the pulse for $c = 2.561340$ and $\delta = 0.13$ (aperiodic regime). The remaining parameters are as in fig.1.

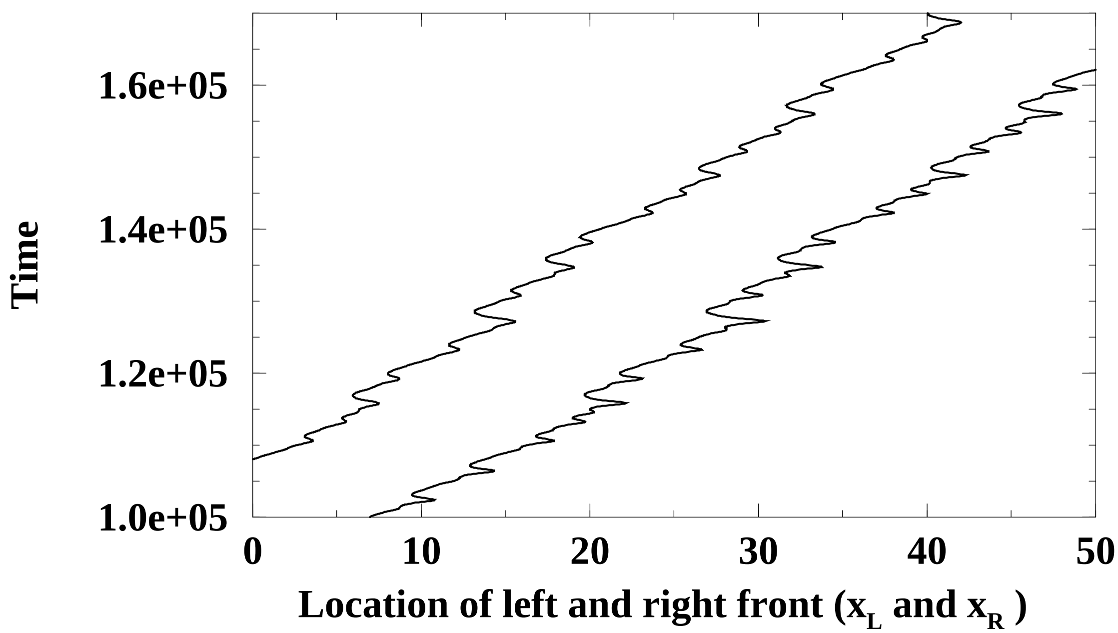

FIG. 5. Space-time diagram of the left and the right front for c = 2.561340 and δ = 0.13 (aperiodic regime). The remaining parameters are as in fig.1.

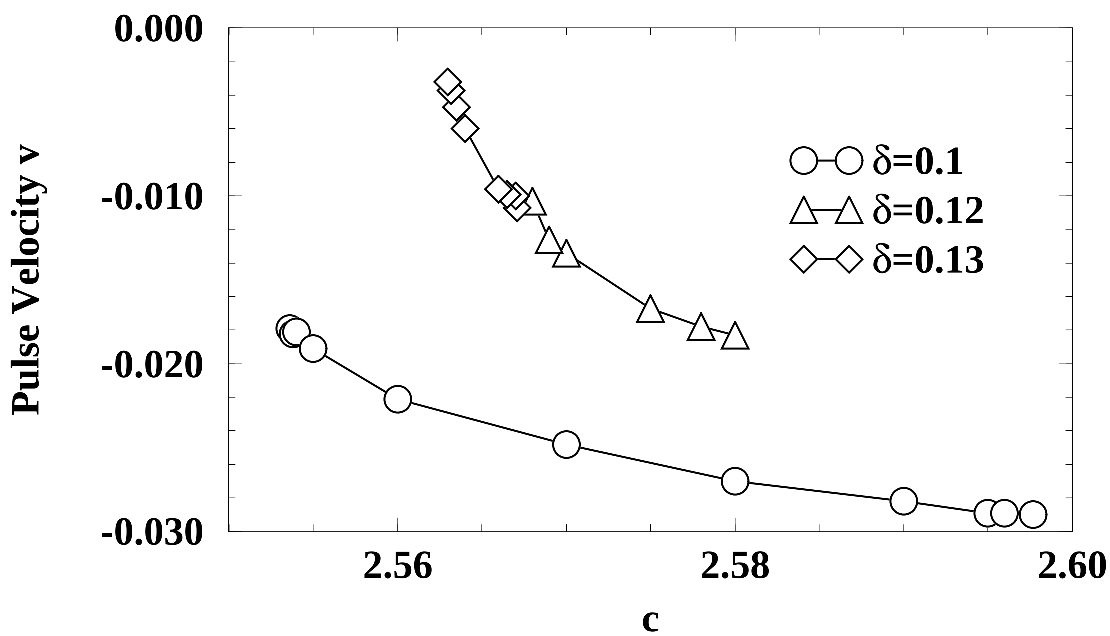

FIG. 6. Velocity of the pulses for different values of the coefficient δ. The remaining parameters are as in fig.1.